Received: 9 June 2020 | Revised: 14 September 2020 | Accepted: 12 October 2020

DOI: 10.1111/cas.14698

ORIGINAL ARTICLE

Cancer Science WILEY

AMP-activated protein kinase activation primes cytoplasmic translocation and autophagic degradation of the BCR-ABL protein in CML cells

Daisuke Koyama[1,2] | Jiro Kikuchi[1] | Yoshiaki Kuroda[1] | Masatsugu Ohta[3] | Yusuke Furukawa[1]

[1]Division of Stem Cell Regulation, Center for Molecular Medicine, Jichi Medical University, Shimotsuke, Japan

[2]Department of Internal Medicine, Fukushima Prefectural Miyashita Hospital, Mishima, Japan

[3]Department of Hematology, Fukushima Medical University Aizu Medical Center, Aizuwakamatsu, Japan

Correspondence
Yusuke Furukawa, Division of Stem Cell Regulation, Center for Molecular Medicine, Jichi Medical University, 3311-1 Yakushiji, Shimotsuke, Tochigi 329-0498, Japan.
Email: furuyu@jichi.ac.jp

Funding information Ministry of Education, Culture, Sports, Science and Technology; Japan Society for the Promotion of Science; Bristol-Myers Squibb; Fukushima Prefectural Hospital Bureau; Novartis Foundation Japan.

Abstract

Chronic myeloid leukemia is driven by the BCR-ABL oncoprotein, a constitutively active protein tyrosine kinase. Although tyrosine kinase inhibitors (TKIs) have greatly improved the prognosis of CML patients, the emergence of TKI resistance is an important clinical problem, which deserves additional treatment options based on unique biological properties to CML cells. In this study, we show that metabolic homeostasis is critical for survival of CML cells, especially when the disease is in advanced stages. The BCR-ABL protein activates AMP-activated protein kinase (AMPK) for ATP production and the mTOR pathway to suppress autophagy. BCR-ABL is detected in the nuclei of advanced-stage CML cells, in which ATP is sufficiently supplied by enhanced glucose metabolism. AMP-activated protein kinase is further activated under energy-deprived conditions and triggers autophagy through ULK1 phosphorylation and mTOR inhibition. In addition, AMPK phosphorylates 14-3-3 and Beclin 1 to facilitate cytoplasmic translocation of nuclear BCR-ABL in a BCR-ABL/14-3-3τ/Beclin1/XPO1 complex. Cytoplasmic BCR-ABL protein undergoes autophagic degradation when intracellular ATP is exhausted by disruption of the energy balance or forced autophagy flux with AMP mimetics, mTOR inhibitors, or arsenic trioxide, leading to apoptotic cell death. This pathway represents a novel therapeutic vulnerability that could be useful for treating TKI-resistant CML.

KEYWORDS

AMPK, autophagy, BCR-ABL, cancer metabolism, mTOR

1 | INTRODUCTION

Chronic myeloid leukemia is a myeloproliferative neoplasm driven by the BCR-ABL tyrosine kinase, the product of the Ph chromosome.[1,2] Tyrosine kinase inhibitors have greatly improved the prognosis of patients with CML[3]; however, at least two problems should be resolved to fulfill unmet medical needs. First, TKI therapy cannot eradicate CML stem cells[2]; therefore,

Abbreviations: 2-NBDG, 2-deoxy-2-[(7-nitro-2,1,3-benzoxadiazol-4-yl) amino]-D-glucose; ACC, acetyl-CoA carboxylase; AICAR, 5-aminoimidazole-4-carboxamide-1-β-D-ribofuranoside; ALL, acute lymphoblastic leukemia; AMPK, AMP-activated protein kinase; ATO, arsenic trioxide; CML-BC, CML in blast crisis; CPT, carnitine palmitoyltransferase; FAO, fatty acid oxidation; GLUT, glucose transporter; LKB1, liver kinase B1; Ph, Philadelphia chromosome; TKI, tyrosine kinase inhibitor; XPO1, exportin 1.

continuous—often lifelong—medication is necessary to sustain remission. In fact, several TKI cessation studies revealed that approximately 50% of patients failed to maintain a deep molecular response after discontinuation of the drug.[4,5] Second, TKIs alone cannot control the disease in advanced stages, such as CML-BC, due to the presence of TKI-resistant mutations of BCR-ABL and additional genetic events.[2,6] These problems prompted us to identify novel therapeutic vulnerabilities whose targeting can synergize with or operate independently of TKIs.

Because of their hyperproliferative nature, CML cells need to generate a sufficient amount of ATP to support cell growth and simultaneously satisfy the anabolic demands of macromolecular biosynthesis.[7,8] To fulfil this requirement, BCR-ABL directly activates the PI3K-AKT pathway to enhance glucose uptake and glycolysis for ATP production,[9] and also activates the mTOR pathway to facilitate protein synthesis and suppress autophagy.[10] In response to a decrease in the intracellular ATP concentration or exposure to metabolic stresses, such as nutrient deprivation and ischemia, the AMPK complex promotes catabolic processes to generate ATP through enhanced glycolysis and FAO, and concomitantly inhibits anabolic processes mainly through phosphorylation of regulatory subunits of mTOR.[11,12] The AMPK-mediated mTOR inhibition could result in the induction of autophagy, which indirectly contributes to ATP production.

Autophagy is an intracellular disposal system, in which cytoplasmic components are degraded by the lysosome.[13] This system is triggered by multiple forms of cellular stress, including nutrient or growth factor deprivation, hypoxia, and DNA damage, and usually acts as a mechanism of cellular defense. In CML cells, however, the autophagic process is suppressed by multiple mechanisms, including AKT-mediated mTOR activation[14] and BCR-ABL-induced Beclin 1 phosphorylation,[15] and is implicated in cell survival and TKI resistance.[16,17] Therefore, forced induction of autophagy could be harmful to CML cells. Indeed, it has been reported that AMPK activators, such as acadesine and metformin, could induce autophagy and subsequent cell death in CML cells[18,19]; however, the mechanism underlying autophagy-associated cell death is not fully understood. In this study, we show that CML cells should halt the initiation of autophagy to prevent autophagic degradation of the BCR-ABL protein. Forced induction of autophagy could be a therapeutic option in TKI-resistant CML.

2 | MATERIALS AND METHODS

2.1 | Cell lines used in the study

We used the following Ph-positive leukemia cell lines: KU812, K562, KOPM28, and TCC-S, established from patients with CML myeloblastic crisis[20,21]; TCC-Y and PALL-2, established from patients with pre-B-cell ALL; KOPM30 and KOPN30bi, established from the same patient with minor BCR gene rearrangement at different stages of the disease; and KOPN66bi, established from a patient with acute mixed lineage leukemia with minor BCR gene rearrangement.[22] Other cell lines were purchased from the Health Science Research Resources Bank, where cell line authenticity and *Mycoplasma* contamination status were routinely checked by DNA fingerprinting and PCR. We undertook genotyping of the BCR-ABL gene using PCR primers shown in Table S1.

2.2 | Exogenous expression of BCR-ABL using retroviral vectors

We purchased the MSCV-(pBabe mcs)-human p210BCR-ABL-IRES-GFP vector from Addgene. Recombinant retrovirus was generated by transfecting the vector into Platinum-A packaging cells (Cell Biolabs) using FuGENE Transfection Reagent (Promega) and transduced into human bone marrow-derived $CD34^+$ cells or human embryonic kidney 293FT cells using ViraDuctin Retrovirus Transduction Reagent (Cell Biolabs).[23]

2.3 | Construction and production of shRNA and CRISPR/Cas9 lentiviral expression vectors

We used the lentiviral shRNA/siRNA expression vector pLL3.7 for knockdown experiments and the lentiCRISPRv2 vector (Addgene), which expresses gRNA and the Cas9 nuclease, for CRISPR/Cas9-mediated deletion of target genes. The oligonucleotides containing the shRNA and CRISPR/Cas9 target sequences are shown in Tables S2 and S3, respectively. After lentiviral transduction, we established stable transformants by isolating single cell clones using limiting dilution (1 cell/well in 96-well culture plates) after long-term culture. The knockdown efficiency was verified by immunoblotting for each clone.

2.4 | Measurement of intracellular ATP concentrations

Total ATP levels were measured using an ATP Bioluminescence Assay Kit CLS II (Sigma-Aldrich). In brief, cells were cultured at 1×10^5 cells/mL under nutrient-rich conditions to exclude the influence of autophagy and resuspended in 50 μL dilution buffer (100 mmol/L Tris-HCl, 4 mmol/L EDTA; pH 7.75), followed by the addition of 450 μL boiling dilution buffer and incubation at 100°C for 2 minutes. After centrifugation, the supernatants were transferred to fresh tubes and immediately subjected to the assay. The ATP concentrations were determined as nmol/L per 10^5 cells by comparison with ATP standards supplied in the kit.

2.5 | Real-time monitoring of ATP production

The rate of ATP production was measured in real time using an Agilent Seahorse XFp Real-Time ATP Rate Assay Kit for the Agilent

Seahorse XFp Extracellular Flux Analyzer (Agilent Technologies). After the assessment of basal respiration, 2×10^4 cells were treated with 40 μg/mL oligomycin, followed by the addition of rotenone and antimycin A at 1 μmol/L each. An oligomycin-induced decrease in the oxygen consumption rate allows the estimation of mitochondrial ATP production. Glycolysis-mediated ATP production is calculated from the proton efflux rate in the presence of rotenone and antimycin, the combination of which completely blocks mitochondrial respiration.

2.6 | Measurement of glucose uptake

We examined the glucose uptake using 2-NBDG, a fluorescent deoxyglucose analog that can be taken up by cells through glucose transporters, supplied in a 2-NBDG Glucose Uptake Assay Kit (BioVision). After being cultured in medium with or without drugs, including imatinib and phloretin, a glucose uptake inhibitor, for 1 hour, cells were pulsed with 2-NBDG and analyzed by flow cytometry or fluorescence microscopy.

2.7 | Immunofluorescence staining and fluorescence microscopy

We generated an anti-BCR-ABL (e14a2) junction-specific Ab for immunocytochemistry by immunizing rabbits with the peptide C + KQSSVPTSSKENLL corresponding to amino acids 78-91 (EU394718.1) of the e14a2-type BCR-ABL protein (Figure S1). Specificity of the antibody was validated by peptide blocking and negative staining of e1a2-type BCR-ABL protein in Ph-positive ALL cells (Figure S2). For immunofluorescent staining, cells were placed on a glass slide using a Cytospin centrifuge (Shandon Scientific) or cultured on a chamber slide and fixed using an Image-iT Fixation/Permeabilization Kit (Thermo Fisher Scientific).[24] These specimens were stained with a rabbit BCR-ABL junction-specific Ab and anti-p62 (MBL), anti-CD34, or anti-pan 14-3-3 (Santa Cruz Biotechnology) Abs. We used Alexa Fluor 594-conjugated anti-rabbit IgG and Alexa Fluor 488-conjugated anti-mouse IgG Abs (Invitrogen) as secondary Abs. Finally, nuclei were counterstained with ProLong Gold Antifade Reagent with DAPI (Cell Signaling Technology). Stained samples were observed under a BZ-X fluorescence microscope (Keyence).

Other conventional techniques and reagents are described in Document S1.

3 | RESULTS

3.1 | BCR-ABL-mediated AMPK activation ensures excessive ATP production in CML cells

It is easy to speculate that CML cells consume a large amount of ATP because the BCR-ABL protein is a constitutively active tyrosine kinase. We confirmed this notion and investigated the mechanisms by which CML cells maintain high intracellular ATP concentrations. First, we cultured various malignant hematopoietic cells under nutrient-rich conditions to inhibit the execution of autophagy, and measured intracellular ATP concentrations with a bioluminescence assay immediately after harvesting. Intracellular ATP levels were significantly higher in CML-BC cell lines (K562, KOPM28, TCC-S, and KU812) than in other BCR-ABL-negative leukemia/lymphoma cell lines (Figure 1A, left panel). Despite their relatively lower intracellular ATP concentrations among the CML-BC group, KOPM28 cells produced more ATP than BCR-ABL nonexpressing cells (Figure S3). Exogenous expression of BCR-ABL significantly increased intracellular ATP concentrations (Figure 1A, middle panel) and mitochondrial respiration (Figure 1A, right panel) in human embryonic kidney 293FT cells, suggesting the direct role of BCR-ABL in active ATP production. Mechanistically, introduction of BCR-ABL increased the abundance of phosphorylated AMPKα and its substrate ACC, which mediates fatty acid synthesis, and upregulated the expression levels of the GLUT1 glucose transporter and CPT1α, a critical regulator of FAO, in 293FT cells (Figure 1B, right panel; Table S4 for data quantification). The BCR-ABL-mediated increase in AMPKα phosphorylation was at least partly mediated by reduced phosphorylation of LKB1 at serine 428, which facilitates the conformational change of AMPKα to an active configuration,[25] although the mechanism of LKB1 dephosphorylation remains to be elucidated (Figure 1B, right panel). In addition, BCR-ABL activated the mTOR pathway, as evidenced by increased phosphorylation of ribosomal protein S6 kinase 1 at serine 411. The same pattern was observed in CML-BC cells but not BCR-ABL-negative Jeko-1 cells: AMPKα was highly phosphorylated at threonine 172 and was thus activated, whereas ACC was highly phosphorylated at serine 79 and was thus inactivated in CML-BC cells (Figure 1B, left panel). These results indicate that BCR-ABL facilitates ATP production through AMPK-mediated activation of FAO and concomitant suppression of fatty acid synthesis as well as through glucose-dependent mechanisms. Intracellular ATP levels were significantly reduced by short-term (24-hour) treatment with the first-in-class TKI imatinib mesylate before the decline in cell viability in CML cells (Figure 1C, left panel). This reduction was associated with a decrease in both the abundance of GLUT1 (Figure 1C, middle panel, and Table S5 for data quantification) and actual glucose uptake (Figure 1D). Time-course studies revealed that the phosphorylation level of AMPKα was transiently declined after BCR-ABL inhibition (2-6 hours) but exceeded the baseline level after 12 hours when intracellular ATP concentrations were <50% of untreated controls (Figure 1C, right panel). These results suggest that AMPKα was compensatorily activated in CML cells in response to imatinib-induced ATP depletion.

3.2 | Prolonged AMPK activation results in energy exhaustion and decreased viability of CML cells

To understand the biological significance of AMPK activation under energy-deprived conditions, we treated TCC-S, KOPM28, and

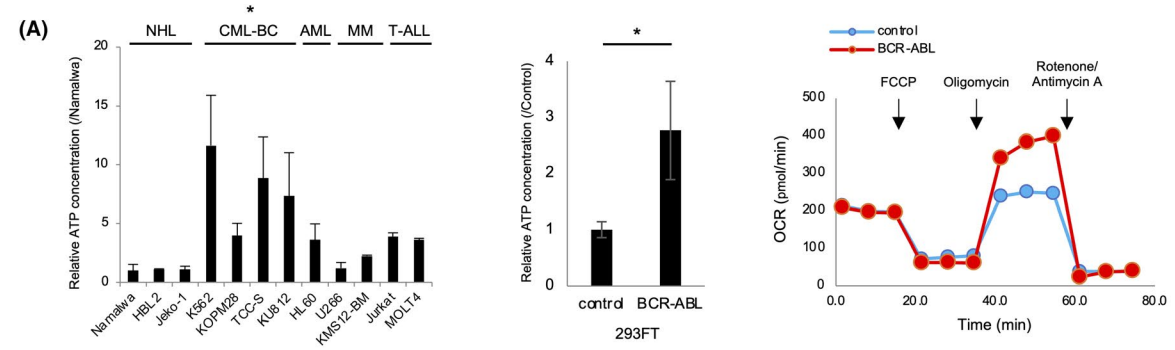
(A)
NHL
CML-BC
AML
MM
T-ALL
Relative ATP concentration (/Namalwa)
Namalwa
HBL-2
Jeko-1
K562
KOPM28
TCC-S
KU812
HL60
U266
KMS12-BM
Jurkat
MOLT4
Relative ATP concentration (/Control)
control
BCR-ABL
293FT
control
BCR-ABL
FCCP
Oligomycin
Rotenone/
Antimycin A
OCR (pmol/min)
Time (min)

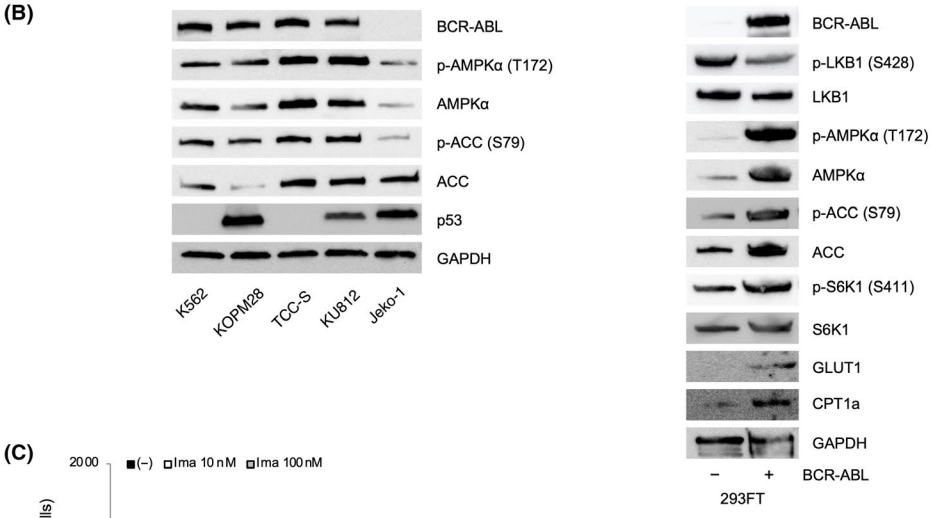
(B)
BCR-ABL
p-AMPKα (T172)
AMPKα
p-ACC (S79)
ACC
p53
GAPDH
K562
KOPM28
TCC-S
KU812
Jeko-1
BCR-ABL
p-LKB1 (S428)
LKB1
p-AMPKα (T172)
AMPKα
p-ACC (S79)
ACC
p-S6K1 (S411)
S6K1
GLUT1
CPT1a
GAPDH
– + BCR-ABL
293FT

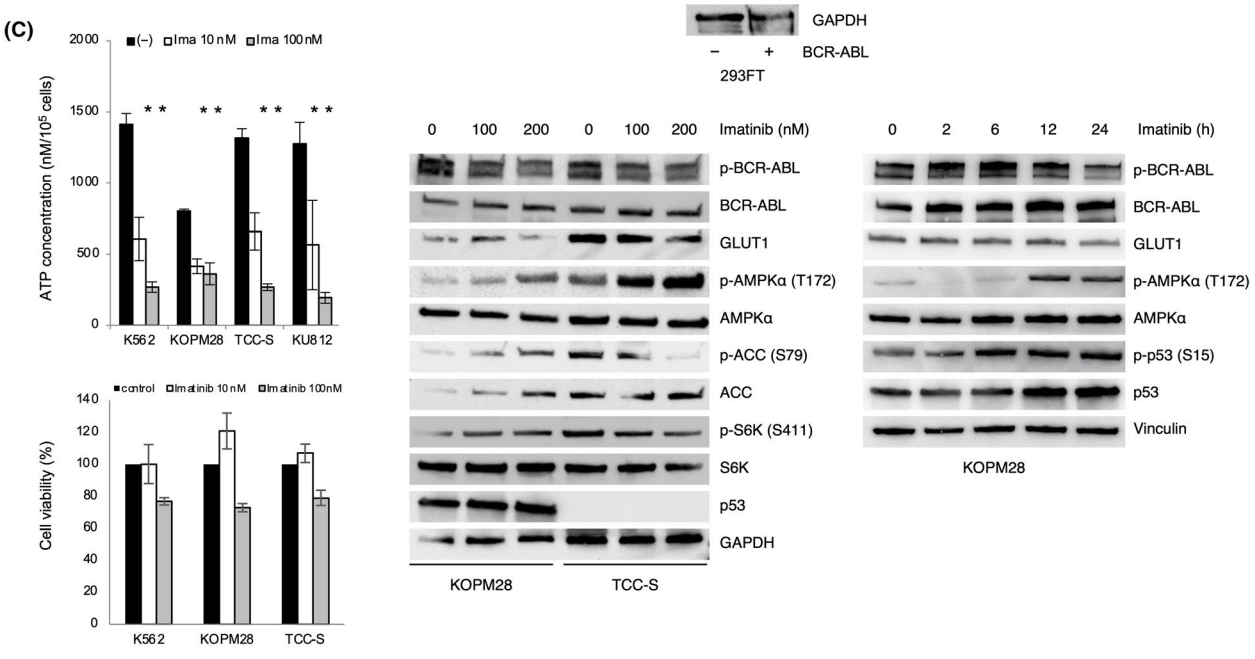
(C)
(–) Ima 10 nM Ima 100 nM
ATP concentration (nM/10⁵ cells)
K562
KOPM28
TCC-S
KU812
control
Imatinib 10 nM
Imatinib 100nM
Cell viability (%)
Imatinib (nM)
Imatinib (h)
p-BCR-ABL
BCR-ABL
GLUT1
p-AMPKα (T172)
AMPKα
p-ACC (S79)
ACC
p-S6K (S411)
S6K
p53
GAPDH
p-p53 (S15)
Vinculin
KOPM28
TCC-S

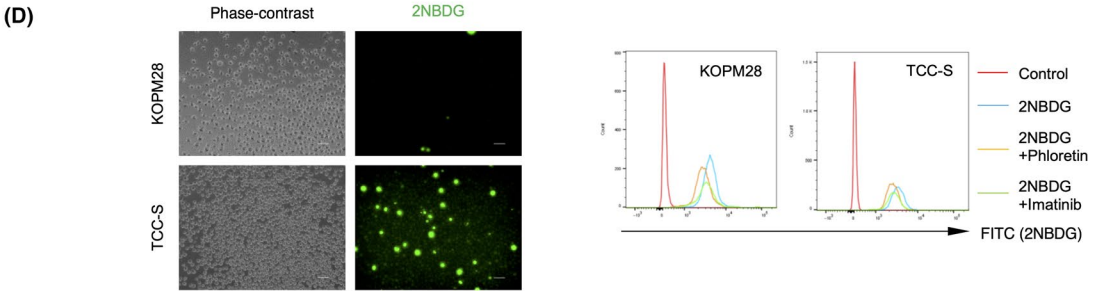
(D)
Phase-contrast
2NBDG
KOPM28
TCC-S
KOPM28
TCC-S
Control
2NBDG
2NBDG
+Phloretin
2NBDG
+Imatinib
FITC (2NBDG)

FIGURE 1 BCR-ABL-mediated AMP-activated protein kinase (AMPK) activation ensures excessive ATP production in CML cells. A, Intracellular ATP concentration was measured using a bioluminescence assay in various hematopoietic cell lines (AML, acute myeloid leukemia; CML-BC, CML in blast crisis; MM, multiple myeloma; NHL, non-Hodgkin lymphoma; T-ALL, T-cell acute lymphoblastic leukemia) (left panel) and BCR-ABL-transduced human embryonic kidney 293FT cells (middle panel) after culture in fresh medium for 24 h. The means ± SD (bars) of the relative ratios compared with Namalwa cells or empty vector-transfected 293FT cells (control) are shown (n = 3). *$P < .05$ between CML-BC and other groups by one-way ANOVA with Tukey's multiple comparison test. The rate of ATP production was measured in empty vector- or BCR-ABL-transfected 293FT cells using the Agilent Seahorse XFp Extracellular Flux Analyzer (right panel). Data shown are representative of three independent experiments. FCCP, carbonyl cyanide-4-phenylhydrazone; OCR, oxygen consumption rate. B, CML-BC and NHL (Jeko-1) cell lines (left panel) or BCR-ABL-transduced 293FT cells (right panel) were cultured in fresh medium for 24 h and subjected to immunoblot analysis of the indicated molecules. C, Left panel, CML cells were cultured with the indicated doses of imatinib mesylate for 24 h and subjected to intracellular ATP measurement (upper) and an MTT reduction assay (lower). Means ± SD (bars) of three independent experiments are shown (*$P < .01$ against untreated controls). Middle panel, CML cells were cultured with the indicated doses of imatinib mesylate for 24 h and subjected to immunoblotting. Right panel, KOPM28 cells were cultured with 50 nmol/L imatinib for the indicated periods and subjected to immunoblotting. D, KOPM28 and TCC-S cells were cultured with 2-deoxy-2-[(7-nitro-2,1,3-benzoxadiazol-4-yl) amino]-D-glucose (2-NBDG) for 30 min and examined under phase-contrast and fluorescence microscopy (left panel) or cultured with 2-NBDG in the absence or presence of either phloretin, a glucose transport inhibitor, or imatinib for 1 h and analyzed by flow cytometry (right panel). ACC, acetyl-CoA carboxylase; CPT1a, carnitine palmitoyltransferase 1α; GLUT1, glucose transporter 1; S6K1, ribosomal protein S6 kinase 1

KOPM28 sublines in which p53 was deleted by CRISPR/Cas9 targeting of TP53 (hereafter defined as KOPM28p53KO) (Figure S4A,B), with AICAR, a small molecule compound capable of activating AMPK as an AMP mimetic.[26] Brief (2-hour) exposure to AICAR significantly enhanced mitochondrial activity and increased intracellular ATP concentrations in all three cell lines (Figure 2A). The AICAR-induced ATP production was sustained for up to 24 hours and returned to the baseline level in KOPM28 cells, in which p53 is mutated in the DNA-binding domain (A276P)[20] but retains the ability to suppress AMPK activity in the cytoplasm[27] (Figure S5). However, ATP levels declined after 24 hours with a loss of mitochondrial function (Figure 2A, middle panel) and cell viability (Figure 2A, left panel) in p53-deficient TCC-S cells. Immunoblotting of subcellular fractions revealed that the phosphorylation level and the cytoplasmic/nuclear localization ratio of AMPKα were higher in TCC-S cells than in KOPM28 cells 2 hours after AICAR treatment, when the intracellular ATP level peaked (Figure 2B). At this stage, no obvious differences were observed in the expression levels of autophagy-initiating proteins, such as ULK1 and p62, between the two cell lines. At the exhaustion phase of AMPK activation (24 hours), the abundance of Beclin 1, p62, and phosphorylated ULK1 was remarkably increased in p53-deficient TCC-S and p53-deleted KOPM28 cells in association with the decrease in cell viability (Figure 2C). These results imply that induction of autophagy is responsible for cell death caused by sustained AMPK activation in CML-BC cells. We then investigated the mechanisms underlying autophagy-induced cell death, which should be unique to CML cells because autophagy is generally cytoprotective.

3.3 | Autophagy is associated with cytoplasmic translocation and subsequent degradation of BCR-ABL protein

It is widely believed that the BCR-ABL protein is localized exclusively in the cytoplasm to promote efficient signal transduction in chronic-phase CML cells.[28,29] The BCR-ABL protein has three nuclear localization signals and only a single nuclear export signal in the c-ABL portion.[30-32] This structure supports the idea that BCR-ABL shuttles between the two cellular compartments in contrast to the current view. Indeed, a substantial portion of BCR-ABL was detected in the nuclei of CML-BC cells (Figure 3A), BCR-ABL-transfected CD34-positive bone marrow mononuclear cells (Figure 3B), and BCR-ABL-transduced 293FT cells (Figure 3C) by immunoblotting of subcellular fractions and immunocytochemistry using a BCR-ABL-specific Ab (Figure S2). Nuclear BCR-ABL protein was translocated to the cytoplasm together with the regulators of intracellular protein localization, XPO1 and 14-3-3, in both CML-BC (Figure 2B) and BCR-ABL-transduced 293FT (Figure 3C) cells following AICAR-induced artificial energy depletion. These results suggest that BCR-ABL resides in the nucleus when ATP supply is sufficient or cellular demand of ATP is relatively low and is translocated to the cytoplasm under energy-deprived conditions for ATP supplementation.

Next, we sought to determine whether cytoplasmic BCR-ABL protein undergoes autophagic degradation in starved CML cells. Treatment of CML-BC cells with ATO, a strong inducer of autophagy,[33] triggered cytoplasmic translocation of BCR-ABL and its subsequent degradation, which was readily suppressed by the lysosomal inhibitor chloroquine (Figure 3D), without a decrease but rather with a compensatory increase in the abundance of BCR-ABL mRNA (Figure S6). Cytoplasmic accumulation of the autophagy proteins Beclin 1 and p62 was concomitantly observed in ATO-treated cells and was also enhanced by chloroquine (Figure 3D). Consistent with a previous attempt using a PROTAC (proteolysis-targeting chimera) against BCR-ABL,[34] BCR-ABL degradation led to immediate death of CML cells (Figure S6). In contrast, the mTOR inhibitor rapamycin alone elicited modest levels of cytoplasmic translocation of BCR-ABL and apoptotic cell death despite the induction of autophagic flux (Figure S7). Furthermore, ATO-treated CML cells did not undergo apoptosis when BCR-ABL degradation was inhibited by shRNA against ULK1 (Figures 4 and S7C). These results suggest that both cytoplasmic translocation and degradation of BCR-ABL are prerequisite for autophagy-associated cell death in CML cells.

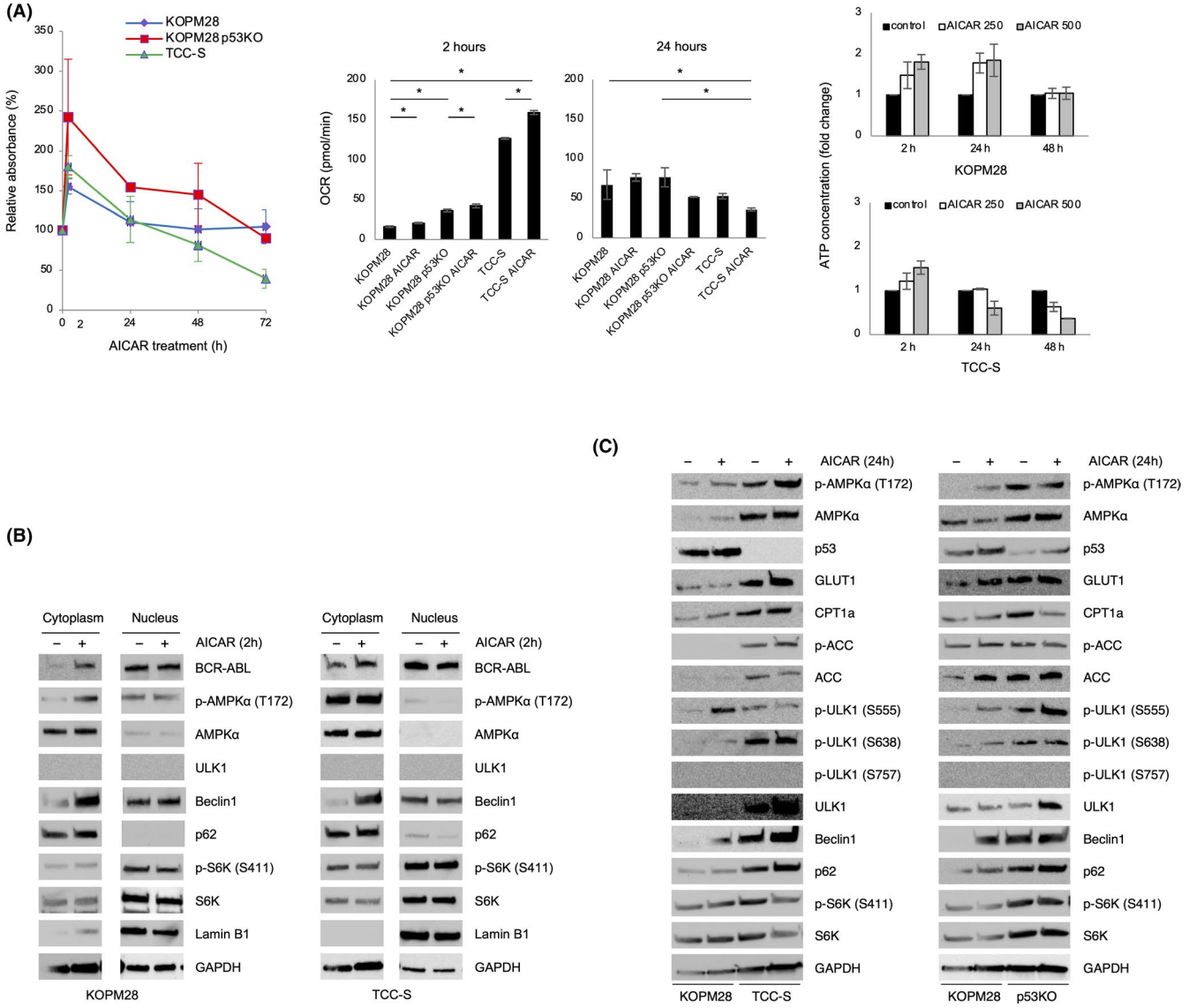

FIGURE 2 Prolonged AMP-activated protein kinase (AMPK) activation results in energy exhaustion and decreased viability of CML cells. A, Left panel, CML cells were cultured with 250 μmol/L 5-aminoimidazole-4-carboxamide-1-β-d-ribofuranoside (AICAR) and subjected to an MTT reduction assay to assess mitochondrial activity and cell viability at the indicated time points. Middle panel, Mitochondrial activity was determined by measuring the oxygen consumption rate (OCR) with the Agilent Seahorse XFp Extracellular Flux Analyzer in CML cells immediately and 24 h after the addition of 250 μmol/L AICAR. Means ± SD (bars) of three independent experiments are shown (*$P < .05$ between the two groups by Student's*ttest). Right panel, The relative concentrations of intracellular ATP were measured in KOPM28 and TCC-S cells cultured with either 250 or 500 μmol/L AICAR for the indicated durations. B, KOPM28 and TCC-S cells were cultured in the absence (–) or presence (+) of 250 μmol/L AICAR for 2 h and expression of the indicated molecules was examined along with Lamin B1 (nuclear marker) and GAPDH (cytoplasmic marker) in the separated cytoplasmic and nuclear fractions. C, KOPM28, TCC-S, and KOPM28p53KO cells were cultured in the absence (–) or presence (+) of 250 μmol/L AICAR for 24 h, and cytoplasmic fractions were isolated for immunoblot analysis of the indicated proteins. ACC, acetyl-CoA carboxylase; CPT1a, carnitine palmitoyltransferase 1α; GLUT1, glucose transporter 1; S6K1, ribosomal protein S6 kinase 1

In previous studies, BCR-ABL localization was examined mostly by immunofluorescent detection of exogenous proteins with Abs against BCR and/or c-ABL.[35-37] However, this experimental system cannot distinguish BCR-ABL from normal BCR and c-ABL proteins derived from residual alleles. To circumvent this issue, we generated a BCR-ABL junction-specific Ab to detect only the e14a2-type BCR-ABL protein by immunocytochemistry (Figure S2). Using the new Ab, we confirmed that BCR-ABL was localized mainly in the nucleus in untreated CML-BC cells (Figures 3E, S8, and S9 for lower-power magnification images). In contrast, BCR-ABL was mostly detected in the cytoplasm in primary CML cells isolated from the bone marrow of chronic-phase patients probably due to p53-mediated energy homeostasis (Figure S10). Nuclear BCR-ABL protein was appreciably translocated to the cytoplasm during autophagic flux induced by ATO (Figure 3E) or the combination of the AMPK activator AICAR and the mTOR inhibitor rapamycin (Figure S11). Colocalization of BCR-ABL and p62 was clearly visualized in CML cells undergoing

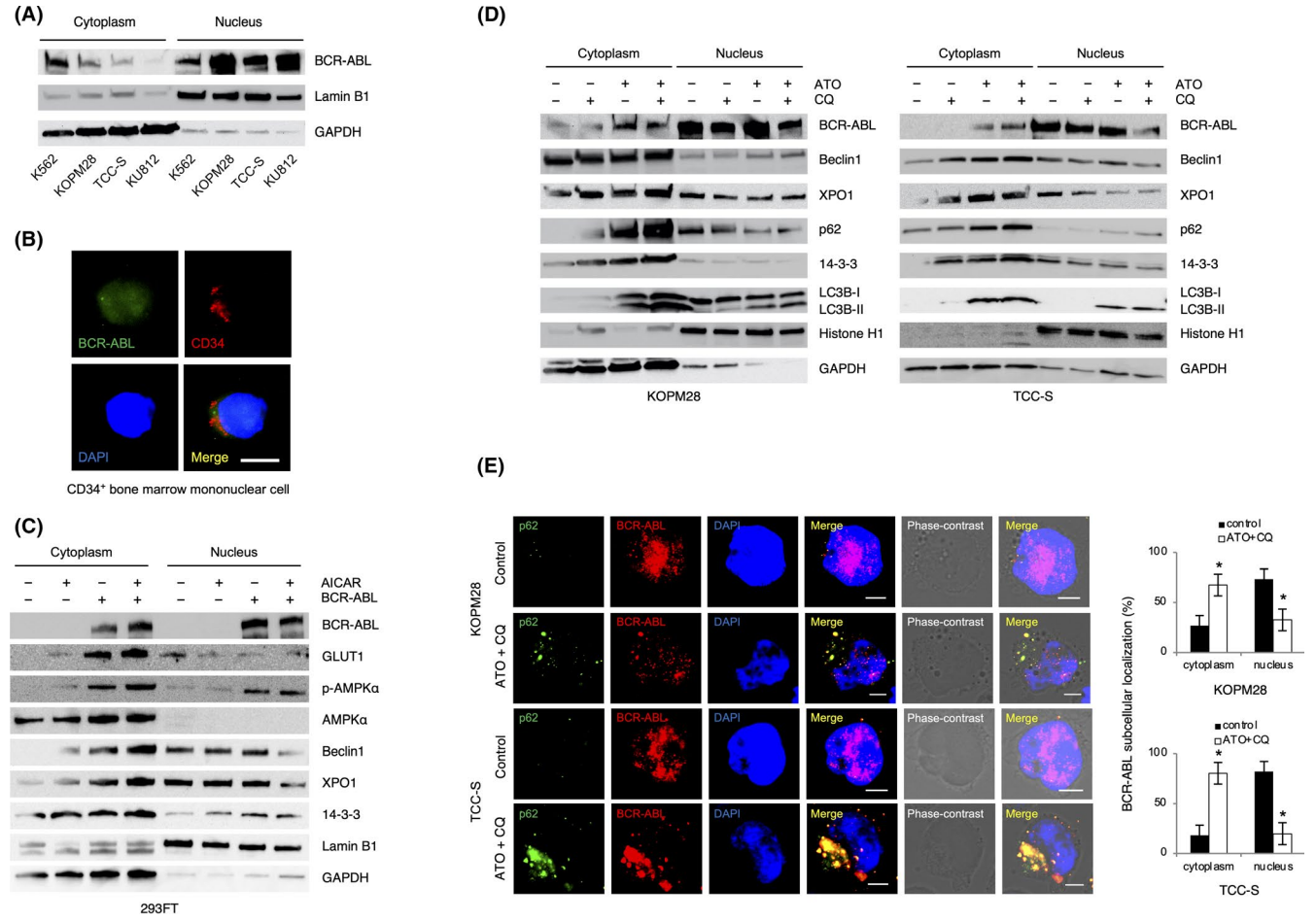

FIGURE 3 Autophagy is associated with cytoplasmic translocation and subsequent degradation of the BCR-ABL protein. A, We isolated the cytoplasmic and nuclear fractions of K562, KOPM28, TCC-S, and KU812 cells cultured under nutrient-rich conditions, and examined the expression of BCR-ABL, Lamin B1, and GAPDH. B, $CD34^+$human bone marrow mononuclear cells were transfected with a BCR-ABL-expression vector and subjected to sequential immunofluorescence staining with the anti-BCR-ABL junction-specific rabbit polyclonal Ab, followed by staining with Alexa Fluor 488-conjugated anti-rabbit IgG (green), and anti-CD34 mouse polyclonal Ab, followed by staining with Alexa Fluor 594-conjugated anti-mouse IgG (red). Nuclei were counterstained with DAPI (blue). Scale line, 50 μm. Data shown are representative of multiple independent experiments. C, Human embryonic kidney 293FT cells were transduced with either empty or BCR-ABL-expression vector, cultured in the absence (–) or presence (+) of 5-aminoimidazole-4-carboxamide-1-β-d-ribofuranoside (AICAR; 250 μmol/L) for 24 h, and subjected to immunoblot analysis of the indicated molecules in the separated cytoplasmic and nuclear fractions. D, KOPM28 and TCC-S cells were cultured with the indicated combinations of arsenic trioxide (ATO; 2.5 μmol/L for KOPM28 and 5 μmol/L for TCC-S) and chloroquine (CQ) (30 μmol/L) for 24 h, and subjected to immunoblot analysis of the indicated molecules in the separated cytoplasmic and nuclear fractions. E, Left panel, KOPM28 and TCC-S cells were cultured in the absence or presence of ATO (2.5 μmol/L for KOPM28 and 5 μmol/L for TCC-S) and CQ (30 μmol/L) for 24 h. Cytospin specimens were stained with the anti-p62 mouse polyclonal Ab, followed by staining with Alexa Fluor 488-conjugated anti-mouse IgG (green), and with anti-BCR-ABL junction-specific rabbit polyclonal Ab, followed by staining with Alexa Fluor 594-conjugated anti-rabbit IgG (red). Nuclei were counterstained with DAPI (blue). Scale bar, 50 μm. Data shown are representative of approximately 30 independent experiments. Right panel, Subcellular localization of BCR-ABL was quantified using BZ-X Analyzer fluorescence microscope software. *$P < .05$ between the control and ATO + CQ treatment by Student'sttest (n = 30). AMPK, AMP-activated protein kinase; GLUT1, glucose transporter 1; XPO1, exportin 1

autophagy when lysosomal degradation of the two proteins was inhibited with chloroquine (Figures 3E and S9).

3.4 | BCR-ABL is translocated from the nucleus in complex with 14-3-3, XPO1, and Beclin 1

Finally, we attempted to clarify the mechanism regulating the subcellular localization of the BCR-ABL protein and its relationship with the priming of autophagy. It has been reported that binding to 14-3-3 proteins disrupts the nuclear localization of the c-Abl protein.[35] As shown in Figure 4A, the BCR-ABL protein harbors six 14-3-3-binding sites: five in the BCR portion and one in the c-ABL portion.[38] The BCR kinase phosphorylates 14-3-3τ,[38] which positively regulates the expression of Beclin 1.[39] Beclin 1 is exported from the nucleus to the cytoplasm in a complex with XPO1 during autophagy.[40] These findings prompted us to examine whether BCR-ABL forms a complex with 14-3-3, XPO1, and Beclin 1 when BCR-ABL is translocated

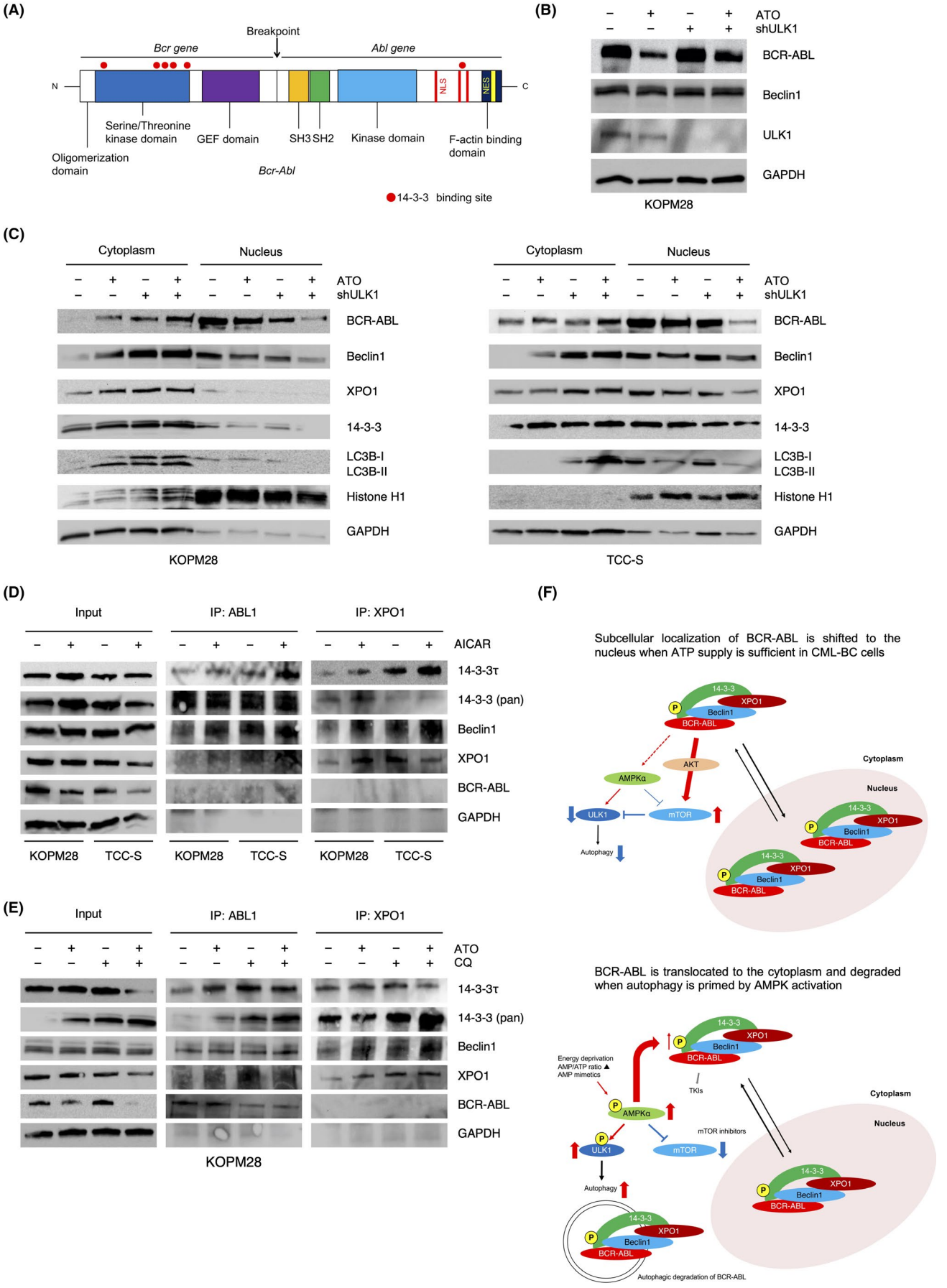
(A)
Breakpoint
Bcr gene
Abl gene
N
C
NLS
NES
Serine/Threonine kinase domain
GEF domain
SH3 SH2
Kinase domain
F-actin binding domain
Oligomerization domain
Bcr-Abl
14-3-3 binding site
(B)
ATO
shULK1
BCR-ABL
Beclin1
ULK1
GAPDH
KOPM28
(C)
Cytoplasm
Nucleus
ATO
shULK1
BCR-ABL
Beclin1
XPO1
14-3-3
LC3B-I
LC3B-II
Histone H1
GAPDH
KOPM28
TCC-S
(D)
Input
IP: ABL1
IP: XPO1
AICAR
14-3-3τ
14-3-3 (pan)
Beclin1
XPO1
BCR-ABL
GAPDH
KOPM28
TCC-S
(E)
Input
IP: ABL1
IP: XPO1
ATO
CQ
14-3-3τ
14-3-3 (pan)
Beclin1
XPO1
BCR-ABL
GAPDH
KOPM28
(F)
Subcellular localization of BCR-ABL is shifted to the nucleus when ATP supply is sufficient in CML-BC cells
14-3-3
XPO1
Beclin1
BCR-ABL
AKT
AMPKα
ULK1
mTOR
Autophagy
Cytoplasm
Nucleus
BCR-ABL is translocated to the cytoplasm and degraded when autophagy is primed by AMPK activation
Energy deprivation
AMP/ATP ratio ▲
AMP mimetics
TKIs
mTOR inhibitors
Autophagic degradation of BCR-ABL

FIGURE 4 BCR-ABL is translocated from the nucleus in complex with 14-3-3, exportin 1 (XPO1), and Beclin 1. A, Structure of the BCR-ABL protein; the red dots indicate the 14-3-3 binding sites. B, KOPM28 cells were lentivirally transduced with either the pLL3.7-sh-control (−) or pLL3.7-sh-ULK1 (+) vector and cultured with 2.0 μmol/L arsenic trioxide (ATO) for 24 h. Whole cell lysates were subjected to immunoblot analysis of the indicated molecules. C, KOPM28 and TCC-S cells were lentivirally transduced with either the pLL3.7-sh-control (−) or pLL3.7-sh-ULK1 (+) vector, and cultured with or without ATO (2.0 μmol/L) for 24 h. The cytoplasmic and nuclear fractions were subjected to immunoblot analysis of the indicated molecules. D, We cultured KOPM28 and TCC-S cells with or without 250 μmol/L 5-aminoimidazole-4-carboxamide-1-β-d-ribofuranoside (AICAR) for 24 h, and extracted whole cell lysates for immunoprecipitation (IP) with anti-c-ABL1 or anti-XPO1 Abs. Immunoprecipitates were analyzed by immunoblotting for the presence of the indicated molecules. E, KOPM28 cells were cultured with the indicated combinations of ATO (2.5 μmol/L) and CQ (30 μmol/L) for 24 h and subjected to the same analysis shown in the panel D. F, Graphical summary of the findings of the present study. AMPK, AMP-activated protein kinase; CML-BC, CML in blast crisis; NES, nuclear export signal; NLS, nuclear localization signal

to the cytoplasm following the induction of autophagy in CML-BC cells. For this purpose, we established KOPM28 and TCC-S sublines in which the initiation of autophagy was halted by shRNA against ULK1 (Figure S4C) to visualize these changes more clearly. As expected, the BCR-ABL protein was not degraded after ATO treatment in ULK1-knockdown cells (Figure 4B). In these cells, BCR-ABL was exported from the nucleus and accumulated in the cytoplasm together with 14-3-3, XPO1, and Beclin 1 (Figure 4C). To confirm complex formation, we undertook immunoprecipitation on whole-cell extracts from AICAR-treated KOPM28 and TCC-S cells with Abs against c-ABL and XPO1, followed by immunoblotting with Abs against 14-3-3, Beclin 1, and BCR-ABL. BCR-ABL directly bound to 14-3-3, particularly 14-3-3τ, and Beclin 1; moreover, it indirectly bound to XPO1 through 14-3-3 (Figure 4D). Notably, AMPK activation enhanced the formation of the complex between BCR-ABL and 14-3-3τ as well as the complex between XPO1 and 14-3-3τ in CML cells. Similarly, both BCR-ABL and XPO1 bound to 14-3-3τ during autophagy induction by ATO treatment (Figures 4E and S12). Morphological examination confirmed the colocalization of BCR-ABL and 14-3-3 in clinical samples from CML patients (Figure S13). These results indicate that AMPK triggers autophagy through phosphorylation of ULK1 and mTOR components, such as Raptor and TSC2, and regulates subcellular localization of BCR-ABL through phosphorylation of cargo proteins 14-3-3 and Beclin 1 (Figure 4F). Balance of the two processes critically determines the fate of CML cells, as exemplified by therapeutic effects of AMPK activation.[18]

4 | DISCUSSION

In this study, we show the functional link between intracellular ATP levels and the subcellular localization of BCR-ABL in CML cells. Chronic myeloid leukemia cells produce a large amount of ATP to suppress the initiation of autophagy and subsequent degradation of BCR-ABL in the cytoplasm. To support the high demand for ATP, BCR-ABL facilitates glucose uptake through AKT-mediated upregulation and stabilization of the GLUT1 and GLUT4 transporters.[41] During the chronic phase of CML, p53 acts as a metabolic gatekeeper to maintain intracellular ATP concentrations at a balanced level for proliferation and differentiation.[42] Under these conditions, cytoplasmic localization is suitable for the BCR-ABL protein to transduce proliferative signals efficiently and generate ATP sufficiently. In CML-BC cells, ATP is overproduced by unlimited AMPK activation due to loss of p53 functions. Because the intracellular ATP concentration is sufficient, BCR-ABL is no longer required to stay in the cytoplasm and thus translocates to the nucleus in CML-BC cells. When energy depletion is imposed on CML-BC cells, for example, through an AICAR-mediated artificial increase in AMP, BCR-ABL returns to the cytoplasm to support the ATP supply and could be degraded by autophagy, which is inevitably activated for urgent energy supplementation, at the expense of intracellular energy equilibrium.

Our data indicate that the subcellular localization of BCR-ABL is actively regulated by the AMPKα-related machinery. AMP-activated protein kinase is constitutively activated in CML cells to remodel the net cellular metabolism toward catabolism.[11] Activation of AMPKα results in increased expression of substrates crucial for the maintenance of intracellular ATP levels, including TXNIP13 and TBC1D1, which stabilize glucose transporters on the cell surface,[43] ACC1/2, which catalyzes the first step of lipid synthesis and the generation of malonyl Co-A to inhibit the FAO regulator CPT1,[43] and TSC2 and Raptor, which negatively regulate mTOR activity to repress protein synthesis and promote autophagy.[44] In addition to targeting metabolic regulators, AMPKα targets the molecules governing the subcellular localization of various cargo proteins. The AMPKα-induced phosphorylation of 14-3-3 enhances the binding of 14-3-3 to BCR-ABL for shuttling between the cytoplasmic and nuclear compartments. Furthermore, AMPK regulates the cytoplasmic translocation of nuclear BCR-ABL by facilitating its binding to XPO1. Indeed, an XPO1 inhibitor, leptomycin B, induces the death of CML cells through nuclear entrapment of BCR-ABL.[45,46] Sustained nuclear localization of BCR-ABL could be harmful to CML cells because of disturbance of proliferative and antiapoptotic signal transduction. Together with our data, these findings suggest that the context-dependent nuclear-cytoplasmic shuttling of BCR-ABL is important for cellular homeostasis in CML. Mutations at the sites regulating subcellular localization, such as the F-actin binding domain, nuclear export signals, and nuclear localization signals (Figure 4A), could direct the nuclear localization of BCR-ABL in CML-BC cells. We excluded this possibility by undertaking targeted sequencing of these regions (data deposited in the DDBJ/EMBL/GenBank database under accession numbers LC493097, LC493098, LC493099, and LC493100).

Autophagy contributes to the elimination of dysfunctional mitochondria and redox-active protein aggregates, which are the source

of genotoxic reactive oxygen species, to maintain genomic stability.[47] Baseline autophagic activity acts to eliminate the byproducts of normal cellular processes to maintain cellular homeostasis.[13] Similarly, autophagic degradation of BCR-ABL triggered by nutrient exhaustion might protect CML cells from acquiring phenotypes promoting disease progression, even if AMPKα is activated to enhance cell growth. This view is compatible with a recent description of autophagic elimination of T315I-mutated BCR-ABL protein.[19] The mTOR pathway is constitutively active in CML cells to synthesize proteins required for cell proliferation and halt the induction of autophagy.[10,29] BCR-ABL degradation occurs when these two processes—activation of AMPKα to regulate the subcellular localization of BCR-ABL and repression of mTOR to promote autophagy—are coupled. Drugs that produce both of these effects are candidates for the treatment of TKI-resistant CML cells. In fact, CML-BC cells underwent BCR-ABL degradation and subsequent cell death when treated with ATO, a canonical autophagy inducer, or the combination of the AMPK activator AICAR and the mTOR inhibitor rapamycin (Figure S11), both of which obviously enhanced the effects of TKIs on CML-BC cells (Figures S14 and S15). Overall, these results point to a novel therapeutic vulnerability that could be useful for treating TKI-resistant CML.

ACKNOWLEDGMENTS

The authors are grateful to Ms Mai Tadaki for her technical assistance. We thank Dr Takeshi Inukai and Dr Kanji Sugita (University of Yamanashi) for providing BCR-ABL-positive cell lines, Dr Noboru Mizushima (University of Tokyo) for providing the autophagic flux probe, and Mr Toru Haga (Aizu Medical Center) for clinical sample collection. This work was supported by the Ministry of Education, Culture, Sports, Science and Technology-supported program for the Strategic Foundation at Private Universities (to YF), a Grant-in-Aid for Scientific Research (C) from JSPS (to DK and YF), a Bristol-Myers Squibb Research Grant (to Y. F.), and a grant from the Fukushima Prefectural Hospital Bureau (to DK). YF was funded by the Novartis Foundation Japan.

DISCLOSURE

The authors have no conflict of interest.

ORCID

Yusuke Furukawa https://orcid.org/0000-0002-7249-6418

REFERENCES

1. Branford S, Kim DDH, Apperley JF, et al. Laying the foundation for genomically-based risk assessment in chronic myeloid leukemia. *Leukemia*. 2019;33:1835-1850.
2. Houshmand M, Simonetti G, Circosta P, et al. Chronic myeloid leukemia stem cells. *Leukemia*. 2019;33:1543-1556.
3. Hochhaus A, Larson RA, Guilhot F, et al. Long-term outcomes of imatinib treatment for chronic myeloid leukemia. *N Engl J Med*. 2017;376:917-927.
4. Kimura S. Current status of ABL tyrosine kinase inhibitors stop studies for chronic myeloid leukemia. *Stem Cell Investig*. 2016;3:36.
5. Kimura S, Imagawa J, Muroi Y, et al. Treatment-free remission after first-line dasatinib discontinuation in patients with chronic myeloid leukaemia (first-line DADI trial): a single-arm, multicentre, phase 2 trial. *Lancet Haematol*. 2020;7:e218-e225.
6. Ko TK, Javed A, Lee KL, et al. An integrative model of pathway convergence in genetically heterogeneous blast crisis chronic myeloid leukemia. *Blood*. 2020;135:2337-2353.
7. Sawyers CL. Shifting paradigms: the seeds of oncogene addiction. *Nat Med*. 2009;15:1158-1161.
8. Cantor JR, Sabatini DM. Cancer cell metabolism: one hallmark, many faces. *Cancer Discov*. 2012;2:881-898.
9. Cilloni D, Saglio G. Molecular pathways: BCR-ABL. *Clin Cancer Res*. 2012;18:930-937.
10. Kim YC, Guan K-L. mTOR: a pharmacologic target for autophagy regulation. *J Clin Invest*. 2015;125:25-32.
11. Herzig S, Shaw RJ. AMPK: guardian of metabolism and mitochondrial homeostasis. *Nat Rev Mol Cell Biol*. 2018;19:121-135.
12. Kazyken D, Magnuson B, Bodur C, et al. AMPK directly activates mTORC2 to promote cell survival during acute energetic stress. *Sci Signal*. 2019;12:eaav3249.
13. Doherty J, Baehrecke EH. Life, death and autophagy. *Nat Cell Biol*. 2018;20:1110-1117.
14. Sheng Z, Ma L, Sun JE, Zhu LJ, Green MR. BCR-ABL suppresses autophagy through ATF5-mediated regulation of mTOR transcription. *Blood*. 2011;118:2840-2848.
15. Yu C, Gorantla SP, Müller-Rudorf A, et al. Phosphorylation of BECLIN-1 by BCR-ABL suppresses autophagy in chronic myeloid leukemia. *Haematologica*. 2020;105:1285-1293.
16. Hirao T, Yamaguchi M, Kikuya M, Chibana H, Ito K, Aoki S. Altered intracellular signaling by imatinib increases the anti-cancer effects of tyrosine kinase inhibitors in chronic myelogenous leukemia cells. *Cancer Sci*. 2018;109:121-131.
17. Mitchell R, Hopcroft LEM, Baquero P, et al. Targeting BCR-ABL-independent TKI resistance in chronic myeloid leukemia by mTOR and autophagy inhibition. *J Natl Cancer Inst*. 2018;110:467-478.
18. Vakana E, Altman JK, Glaser H, Donato NJ, Platanias LC. Antileukemic effects of AMPK activators on BCR-ABL-expressing cells. *Blood*. 2011;118:6399-6402.
19. Shinohara H, Minami Y, Naoe T, Akao Y. Autophagic degradation determines the fate of T315I-mutated BCR-ABL protein. *Haematologica*. 2019;104:e191-e194.
20. Takagi M, Shigeta T, Asada M, et al. DNA damage-associated cell cycle and cell death control is differentially modulated by caffeine in clones with p53 mutations. *Leukemia*. 1999;13:70-77.
21. Kano Y, Akutsu M, Tsunoda S, et al. In vitro cytotoxic effects of a tyrosine kinase inhibitor STI571 in combination with commonly used antileukemic agents. *Blood*. 2001;97:1999-2007.
22. Kuroda I, Inukai T, Zhang X, et al. BCR-ABL regulates death receptor expression for TNF-related apoptosis-inducing ligand (TRAIL) in Philadelphia chromosome-positive leukemia. *Oncogene*. 2013;32:1670-1681.
23. Wada T, Koyama D, Kikuchi J, Honda H, Furukawa Y. Overexpression of the shortest isoform of histone demethylase LSD1 primes hematopoietic stem cells for malignant transformation. *Blood*. 2015;125:3731-3746.
24. Kikuchi J, Koyama D, Wada T, et al. Phosphorylation-mediated EZH2 inactivation promotes drug resistance in multiple myeloma. *J Clin Invest*. 2015;125:4375-4390.
25. Kawashima I, Mitsumori T, Nozaki Y, et al. Negative regulation of the LKB1/AMPK pathway by ERK in human acute myeloid leukemia cells. *Exp. Hematol*. 2015;43:524-533.
26. Dembitz V, Lalic H, Visnjic D. 5-Aminoimidazole-4-carboxamide ribonucleoside-induced autophagy flux during differentiation of monocytic leukemia cells. *Cell Death Discov*. 2017;3:17066.

27. Zhou GE, Wang J, Zhao M, et al. Gain-of-function mutant p53 promotes cell growth and cancer cell metabolism via inhibition of AMPK activation. *Mol Cell*. 2014;54:960-974.
28. Patel H, Marley SB, Greener L, Gordon MY. Subcellular distribution of $p210^{BCR-ABL}$ in CML cell lines and primary $CD34^{+}$ CML cells. *Leukemia*. 2008;22:559-571.
29. Dong S, Kang S, Lonial S, Khoury HJ, Viallet J, Chen J. Targeting 14-3-3 sensitizes native and mutant BCR-ABL to inhibition with U0126, rapamycin and Bcl-2 inhibitor GX15-070. *Leukemia*. 2008;22:572-577.
30. Van Etten RA, Jackson P, Baltimore D. The mouse type IV c-abl gene product is a nuclear protein, and activation of transforming ability is associated with cytoplasmic localization. *Cell*. 1989;58:669-678.
31. Taagepera S, McDonald D, Loeb JE, et al. Nuclear-cytoplasmic shuttling of C-ABL tyrosine kinase. *Proc Natl Acad Sci USA*. 1998;95:7457-7462.
32. Yoshida K, Yamaguchi T, Natsume T, Kufe D, Miki Y. JNK phosphorylation of 14-3-3 proteins regulates nuclear targeting of c-Abl in the apoptotic response to DNA damage. *Nat Cell Biol*. 2005;7:278-285.
33. Goussetis DJ, Gounaris E, Wu EJ, et al. Autophagic degradation of the BCR-ABL oncoprotein and generation of antileukemic responses by arsenic trioxide. *Blood*. 2012;120:3555-3562.
34. Lai AC, Toure M, Hellerschmied D, et al. Modular PROTAC design for the degradation of oncogenic BCR-ABL. *Angew Chem Int Edit*. 2016;55:807-810.
35. Wertheim JA, Perera SA, Hammer DA, Ren R, Boettiger D, Pear WS. Localization of BCR-ABL to F-actin regulates cell adhesion but does not attenuate CML development. *Blood*. 2003;102:2220-2228.
36. Li Q, Huang Z, Gao M, et al. Blockade of Y177 and nuclear translocation of Bcr-Abl inhibits proliferation and promotes apoptosis in chronic myeloid leukemia cells. *Int J Mol Sci*. 2017;18:537.
37. Nie D, Huang K, Yin S, et al. KPT-330 inhibition of chromosome region maintenance 1 is cytotoxic and sensitizes chronic myeloid leukemia to Imatinib. *Cell Death Discov*. 2018;4:48.
38. Clokie SJ, Cheung KY, Mackie S, Marquez R, Peden AH, Aitken A. BCR kinase phosphorylates 14-3-3 Tau on residue 233. *FEBS J*. 2005;272:3767-3776.
39. Wang B, Ling S, Lin WC. 14-3-3τ regulates beclin 1 and is required for autophagy. *PLoS One*. 2010;5:e10409.
40. Liang XH, Yu J, Brown K, Levine B. Beclin 1 contains a leucine-rich nuclear export signal that is required for its autophagy and tumor suppressor function. *Cancer Res*. 2001;61:3443-3449.
41. Schwartzenberg-Bar-Yoseph F, Armoni M, Karnieli E. The tumor suppressor p53 down-regulates glucose transporters GLUT1 and GLUT4 gene expression. *Cancer Res*. 2004;64:2627-2633.
42. Labuschagne CF, Zani F, Vousden KH. Control of metabolism by p53 – cancer and beyond. *Biochim Biophys Acta Rev Cancer*. 2018;1870:32-42.
43. Chan LN, Chen Z, Braas D, et al. Metabolic gatekeeper function of B-lymphoid transcription factors. *Nature*. 2017;542:479-483.
44. Kim J, Kundu M, Viollet B, Guan KL. AMPK and mTOR regulate autophagy through direct phosphorylation of Ulk1. *Nat Cell Biol*. 2011;13:132-141.
45. Vigneri P, Wang JYJ. Induction of apoptosis in chronic myelogenous leukemia cells through nuclear entrapment of BCR-ABL tyrosine kinase. *Nat Med*. 2001;7:228-234.
46. Aloisi A, Di Gregorio S, Stagno F, et al. BCR-ABL nuclear entrapment kills human CML cells: ex vivo study on 35 patients with the combination of imatinib mesylate and leptomycin B. *Blood*. 2006;107:1591-1598.
47. Rybstein MD, Bravo-San Pedro JM, Kroemer G, Galluzzi L. The autophagic network and cancer. *Nat Cell Biol*. 2018;20:243-251.

SUPPORTING INFORMATION

Additional supporting information may be found online in the Supporting Information section.

How to cite this article: Koyama D, Kikuchi J, Kuroda Y, Ohta M, Furukawa Y. AMP-activated protein kinase activation primes cytoplasmic translocation and autophagic degradation of the BCR-ABL protein in CML cells. *Cancer Sci*. 2021;112:194–204. https://doi.org/10.1111/cas.14698